Journal of Alloys and Compounds 515 (2012) 154–160

Contents lists available at SciVerse ScienceDirect

Journal of Alloys and Compounds

journal homepage: www.elsevier.com/locate/jallcom

Structural relaxation and its influence on the elastic properties and notch toughness of Mg–Zn–Ca bulk metallic glass

Yuan-Yun Zhao[a,b,*], Xu Zhao[a]

[a] Shenyang National Laboratory for Materials Science, Institute of Metal Research, Chinese Academy of Sciences, 72 Wenhua Road, Shenyang 110016, China
[b] Zhejiang Province Key Laboratory of Magnetic Materials and Application Technology, Key Laboratory of Magnetic Materials and Devices, Ningbo Institute of Materials Technology & Engineering, Chinese Academy of Sciences, 519 Zhuangshi Road, Zhenhai District, Ningbo, 315201, China

ARTICLE INFO

Article history:
Received 23 October 2011
Received in revised form
22 November 2011
Accepted 24 November 2011
Available online 2 December 2011

Keywords:
Mg-based metallic glass
Biodegradable materials
Structural relaxation
Elastic properties
Notch toughness

ABSTRACT

Structural relaxation and its influence on the elastic properties and mechanical properties of Mg–Zn–Ca bulk metallic glass (BMG) were investigated. It was found that relaxation can occur spontaneously even at room temperature (T_R) because of the high homologous temperature ($T_R/T_g > 0.7$) of the BMG. A linear dependence between enthalpy change (ΔH_t) and free volume change (Δv_f) for the annealed $Mg_{66}Zn_{30}Ca_4$ BMG over a wide temperature range was discovered. The structural relaxation of the $Mg_{66}Zn_{30}Ca_4$ BMG resulted in increased shear modulus μ (3.4%) and decreased Poisson's ratio ν (1.4%). However, the tested BMG samples exhibited no obvious degradation of notch toughness (K_Q) even after full structural relaxation. The K_Q values are 9.0 ± 1.7 MPam$^{1/2}$ and 7.1 ± 1.8 MPam$^{1/2}$ for the freshly prepared samples (annealed at T_R for 1.5 h) and fully relaxed samples (annealed at 373 K for 4 h), respectively. These results indicate that the mechanical properties of the $Mg_{66}Zn_{30}Ca_4$ BMG are not very sensitive to its structural relaxation over a wide temperature and time range. These findings may facilitate the clinical applications of $Mg_{66}Zn_{30}Ca_4$ BMG as a promising implant material for future clinical applications.

1. Introduction

Compared with the commonly used metallic biomaterials, such as stainless steels, titanium, and cobalt–chromium-based alloys, magnesium alloys have attracted considerable attention as potential implant materials in recent years [1–8]. Interest in magnesium alloys have been particularly growing because of their good mechanical properties, excellent biocompatibilities, and biodegradation properties. First, magnesium alloys have lower values of elastic modulus (41–45 GPa) and density (1.7–2.0 g/cm^3) that are closer to those of natural bone than other commonly used metallic implants. Moreover, magnesium alloys are soluble and can be absorbed by the human body, which can prevent a second surgical procedure when they are used as implant devices [4]. However, the practical use of these biocompatible magnesium alloys still face challenges. One major obstacle is its rapid corrosion/degradation rates in physiological conditions (including human body fluid or blood plasma), which leads to rapid loss of strength before the tissue has sufficiently healed [2,4,7]. Another obstacle is the release of hydrogen gas upon degradation which delays healing of the surgical region and leads to necrosis of the tissues because the gas pockets can cause separation of tissues and tissue layers [2–3]. Thus, it is important to explore new types of magnesium-based biomaterials with good mechanical properties, low corrosion rates, and uniform corrosion properties for successful clinical applications of these biomaterials.

Magnesium-based bulk metallic glasses (BMGs) attract interest because of their single-phase and chemically homogeneous alloy system, which may improve the mechanical properties and corrosion resistance of the biomaterials as well as result in more uniform corrosion properties than their crystalline counterparts [9,10]. Among these Mg-based BMGs, Mg–Zn–Ca BMGs containing the essential elements Zn and Ca for humans have recently attracted research interest because of the biosafety and biocompatibility of the released alloying elements. It has been reported that Mg–Zn–Ca metallic glasses not only have high specific strength (250–300 MPa cm^3/g) and high reliability of fracture strength [11,12], but also show lower degradation/corrosion rate and better tissue compatibility than their crystalline counterparts [13]. In particular, there is no clinically observable hydrogen-forming bubble-release during the degradation process of the Mg–Zn–Ca metallic glass implants when the alloys contain a high proportion of Zinc [14] (>28 at%). These advantages make Mg–Zn–Ca metallic glasses an appropriate choice for Mg-based biodegradable materials.

However, the metallic glass obtained from the melt via the rapid solidification technique is essentially in a metastable state, with some additional properties, such as enthalpy and entropy, trapped during its formation process. This behavior enables it to have a tendency to transform into a more stable state through structural

* Corresponding author. Tel.: +86 574 87617212; fax: +86 574 87911392.
E-mail address: zhaoyy@nimte.ac.cn (Y.-Y. Zhao).

0925-8388/$ – see front matter © 2011 Elsevier B.V. All rights reserved.
doi:10.1016/j.jallcom.2011.11.125

relaxation when it is subjected to isothermal annealing at a temperature close to the glass transition temperature (T_g) for a sufficiently long time [15].

Structural relaxation usually results in severe embrittlement for most of the metallic glasses [16–19]. Recently, the discovery of metallic glasses with very low T_g [close to room temperature (T_R)], such as Mg- and Ce-based metallic glasses, have initiated new interest, because structural relaxation may induce embrittlement in these alloys even at T_R, thereby causing concerns about their potential applications [20–24]. However, given the low T_g of the biodegradable Mg–Zn–Ca metallic glasses, whether structural relaxation can occur near T_R and thus induce severe embrittlement have not been well understood so far.

In this work, the $Mg_{66}Zn_{30}Ca_4$ BMG with the highest glass-forming ability (D_c = 5 mm [12]) in a Mg–Zn–Ca system near the Mg corner was fabricated. The structural relaxation at T_R and elevated temperature as well as its influence on free volume change (Δv_f), elastic properties, and mechanical properties of the $Mg_{66}Zn_{30}Ca_4$ BMG were investigated. The possible mechanisms of these behaviors were also discussed.

2. Experimental details

A mixture of pure elements (>99.9 wt.%) of Mg, Ca, and Zn were melted under an inert atmosphere in an induction furnace with the nominal composition of $Mg_{66}Zn_{30}Ca_4$ (in atomic percentage). The master alloy was remelted in a tilting crucible and subsequently cast into the copper mold with an internal rod-shaped cavity of 2.4 mm diameter and 40 mm length. The cross-sectional surfaces of the as-cast and annealed rods were analyzed via X-ray diffraction (XRD) using a Rigaku D/max 2400 diffractometer with monochromated Cu K_α radiation. The glass transition behaviors of the BMGs annealed at T_R and elevated temperature for different periods of time were investigated using a Perkin-Elmer differential scanning calorimeter (DSC-Diamond) under flowing purified argon with a heating rate of 20 K/min. The samples were contained in graphite pans and the temperature measurements were reproducible within an error of ±1 K. The elastic properties of the BMG samples were determined using resonant ultrasound spectroscopy (Quasar, Albuquerque, NM). Samples with an aspect ratio of approximately 0.8 to 1 were placed in the middle of two piezoelectric transducers. Two independent elastic constants C11 and C44 were obtained for calculating the elastic moduli, including Young's modulus (E), shear modulus (μ), bulk modulus (B), and Poisson's ratio (ν). The uncertainties in the calculated values of μ, B, ν, and E were less than ±0.6%. For each relaxed state, at least three carefully prepared cylindrical samples with diameters of 2.4 mm were examined. The density of the as-cast and annealed samples were measured using the Archimedes method in purified water at room temperature, and the effective resolution for the density measurement is ±0.0005 g/cm^3. Through the whole process of density measurement for the different relaxed states, the same bulk sample with an approximate weight of 1 g was used. The micro-hardness test was performed with a Mitutoyo MVK-H3 hardness tester using a 200 g load and 10 s loading time. The average value for micro-hardness was obtained from 15 individual measurements. The samples for notch toughness measurement were obtained from the as-cast and annealed BMG rods with diameters of 2.4 mm. The three-point single edge-notched bend tests, fixed at 20 mm span samples, were performed on an Instron 5848 micro mechanical tester under a displacement control of 0.1 mm/min. Notches with a root radius of about 150 μm were cut to a depth nearly half of the rod diameter using a diamond wire saw. At least eight samples were tested at each relaxed state to ensure that the results were reproducible. The stress intensity factor for the cylindrical configuration was evaluated using the analysis method proposed by Murakami [25]. The toughness values obtained were reported as K_Q instead of valid K_{IC} (plane-strain fracture toughness) because of the absence of a fatigue pre-crack and nonstandard specimen geometries. Nonetheless, K_Q data are still meaningful to distinguish the variation in toughness of the materials under identical testing conditions. The fracture surfaces of the failure samples after three-point bending (3PB) tests were examined in a Quanta 600 scanning electron microscope (SEM).

3. Results and discussion

3.1. Structural relaxation

The enthalpy of glass at a certain temperature below T_g may deviate from its equilibrium value (ΔH^{eq}), because some additional enthalpy can be trapped when the glass forms. The annealing of the glass at a temperature close to T_g for a sufficiently long time will result in the loss of this additional enthalpy and make the glass gradually relax into its equilibrium state. The enthalpy of the glass lost during the isothermal annealing process can be recovered by a subsequent DSC scan of the annealed sample, resulting in an overshoot in the DSC signal in reference to the unrelaxed sample. Hence, the enthalpy of recovery (ΔH_t) during the DSC scan is equal to the enthalpy of relaxation during the isothermal annealing experiment, and the enthalpy of relaxation can be studied by surveying the ΔH_t dependent on the annealing time [26]. Fig. 1 shows a series of DSC scans with a heating rate of 20 K/min for the $Mg_{66}Zn_{30}Ca_4$ BMG annealed at T_R for different time points (curves a–g). An overshoot in the DSC heat flow signal, depending on annealing time, can be clearly observed, indicating that the annealed samples underwent structural relaxation, which progressively lowered the enthalpy content with respect to the as-cast sample. Fig. 2 shows the corresponding ΔH_t for the $Mg_{66}Zn_{30}Ca_4$ BMG by annealing at T_R with different annealing time (t). ΔH_t for a given annealing time was determined from the area between the DSC curve of the relaxed sample and the as-cast sample in Fig. 1. It can be seen that the ΔH_t increases gradually in magnitude with increasing t, and the ΔH_t was measured at 0.46 kJ/mol for the sample that annealed at T_R for 21,800 h (2.5 years). However, because the fully relaxed state by annealing at T_R for $Mg_{66}Zn_{30}Ca_4$ BMG needs an annealing time longer than 2.5 years, the ΔH^{eq} at T_R could not be obtained in the experiment. In order to get the fully relaxed state of the

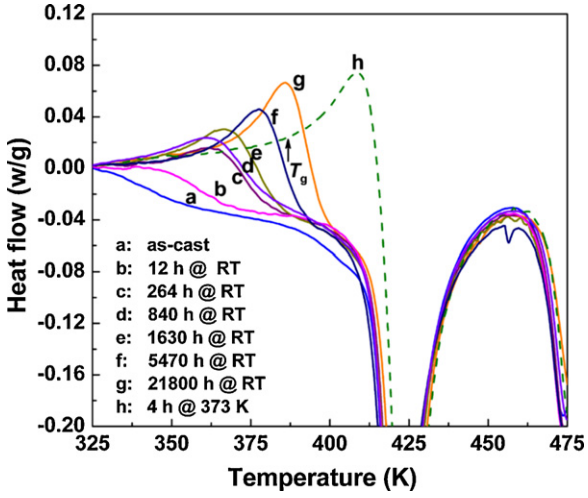

Fig. 1. DSC scans performed with a heating rate of 20 K/min for $Mg_{66}Zn_{30}Ca_4$ BMG by isothermal annealing at room temperature (T_R) for different time (curves a–g) and annealing at 373 K for 4 h (curve h).

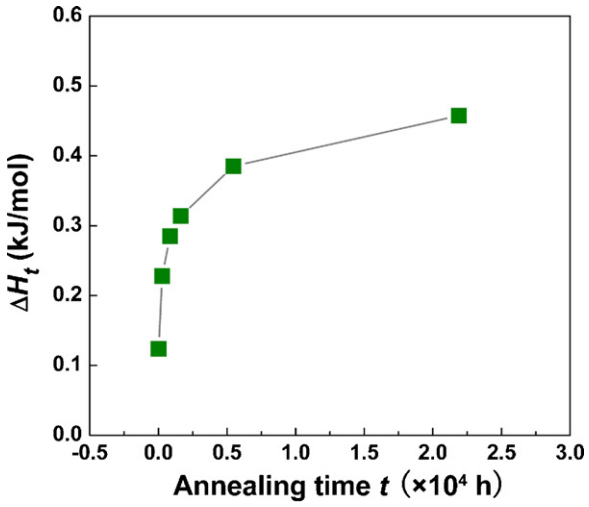

Fig. 2. Correlation between enthalpy change (ΔH_t) and annealing time (t) for the $Mg_{66}Zn_{30}Ca_4$ BMG annealed at room temperature.

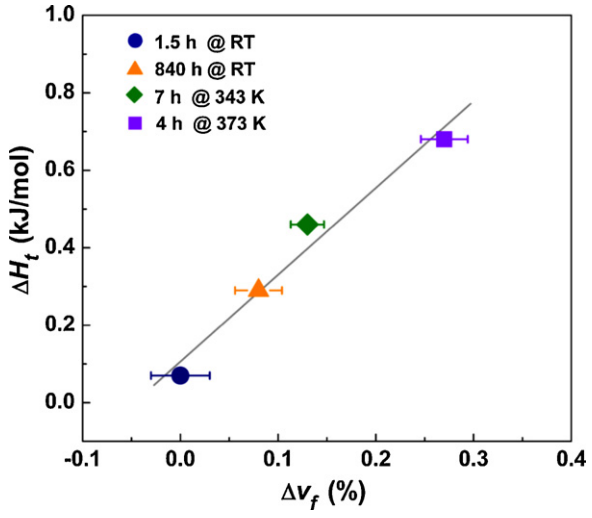

Fig. 4. Enthalpy change (ΔH_t) versus free volume reduction (Δv_f) of the $Mg_{66}Zn_{30}Ca_4$ BMG at different relaxed states.

$Mg_{66}Zn_{30}Ca_4$ BMG at an elevated temperature, the structural relaxation at 373 K (100 °C) was also investigated. Curve h in Fig. 1 shows the DSC scan for a fully relaxed $Mg_{66}Zn_{30}Ca_4$ sample by annealing at 373 K for 4 h, given that there is no change in ΔH_t by further annealing. The ΔH^{eq} at 373 K was measured as 0.68 kJ/mol. As shown in Fig. 1, for the fully relaxed sample at 373 K where relaxation no longer occurs in the DSC experiment, a clear glass transition temperature T_g for $Mg_{66}Zn_{30}Ca_4$ BMG can be determined at 387 K, indicating a high homologous temperature ($T_R/T_g = 0.77$) even at room temperature. Moreover, besides the similar DSC curves during crystallization for the as-cast and fully relaxed sample in Fig. 1, the glass state of the fully relaxed sample at 373 K were also confirmed by the XRD patterns in Fig. 3. No distinct peak corresponding to any crystalline phases can be seen in the diffraction pattern, indicating that the 4 h-annealed sample at 373 K was not crystallized but only structurally relaxed.

3.2. Free volume and elastic properties

To investigate the influence of structural relaxation on the elastic properties and mechanical properties of the $Mg_{66}Zn_{30}Ca_4$ BMG,

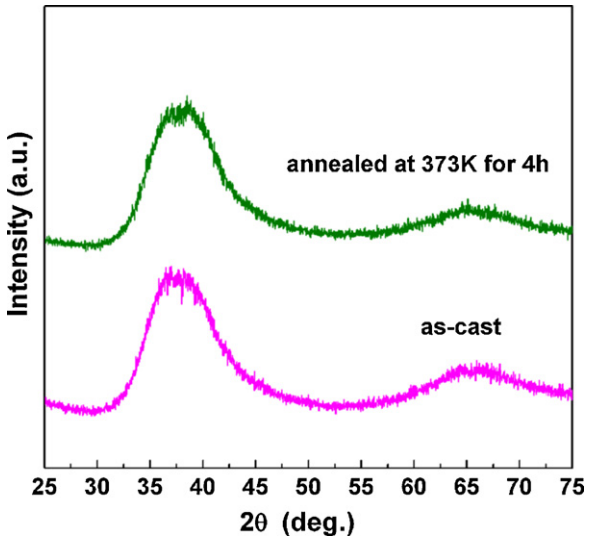

Fig. 3. XRD patterns of the as-cast and fully relaxed $Mg_{66}Zn_{30}Ca_4$ BMG annealed at 373 K for 4 h.

four relaxed-state samples that were annealed at T_R for 1.5 h and 840 h, 343 K for 7 h, and 373 K for 4 h with the corresponding ΔH_t of 0.07 kJ/mol, 0.29 kJ/mol, 0.46 kJ/mol, and 0.68 kJ/mol, respectively, were investigated. The sample annealed at 343 K for 7 h was noted to have a similar enthalpy change value ($\Delta H_t = 0.46$ kJ/mol) with the samples annealed at T_R for 21,800 h. The sample annealed at 373 K for 4 h was fully relaxed.

The change in mass density of the annealed metallic glass is caused by the change in free volume [27,28]. Thus, the change in free volume per atomic volume (Δv_f) for the relaxed sample can be calculated as

$$\Delta v_f = \frac{(\rho_i - \rho_0)}{\rho_0}, \quad (1)$$

where ρ_0 is density of the as-cast sample and ρ_i is density of the relaxed sample.

Fig. 4 displays a plot of ΔH_t against Δv_f for the four relaxed-state samples. Considering that more time is needed to complete the measurement of the mass density for the as-cast samples at T_R, Δv_f is a relative value compared with the sample annealed at T_R for 1.5 h with an initial specific volume of 0.3424 ± 0.0001 cm^3/g. As ΔH_t increases from 0.07 kJ/mol to 0.29 kJ/mol, 0.46 kJ/mol, and 0.68 kJ/mol, the corresponding Δv_f is approximately 0.08%, 0.13%, and 0.27%, respectively, showing a free volume shrinking trend by structural relaxation.

As suggested by van den Beukel and J. Eckert [27,28], there is a linear dependence between ΔH_t and Δv_f:

$$\Delta H_t = \beta \cdot \Delta v_f, \quad (2)$$

where β is a constant.

In the current experiment, the linear fit of ΔH_t versus Δv_f for the $Mg_{66}Zn_{30}Ca_4$ BMG at different relaxed states presented in Fig. 4 yields $\beta = 225$ kJ/mol. Similar to $Zr_{55}Cu_{30}Al_{10}Ni_5$ BMG, there is also no distinct difference between T_R and high temperature structural relaxation [28]. The enthalpy change during structural relaxation was accompanied by a free volume reduction with the same proportionality constant. Thus, the degree of structural relaxation for the $Mg_{66}Zn_{30}Ca_4$ BMG annealed at a different temperature with different annealing time can be well evaluated by the magnitude of Δv_f.

Accordingly, Fig. 5 displays the shear modulus (μ) and Poisson's ratio (ν) as a function of Δv_f for the $Mg_{66}Zn_{30}Ca_4$ BMG at different relaxed states. As shown in Fig. 5, the sample annealed at T_R for 1.5 h exhibits the highest ν of 0.299 ± 0.001 and the lowest μ

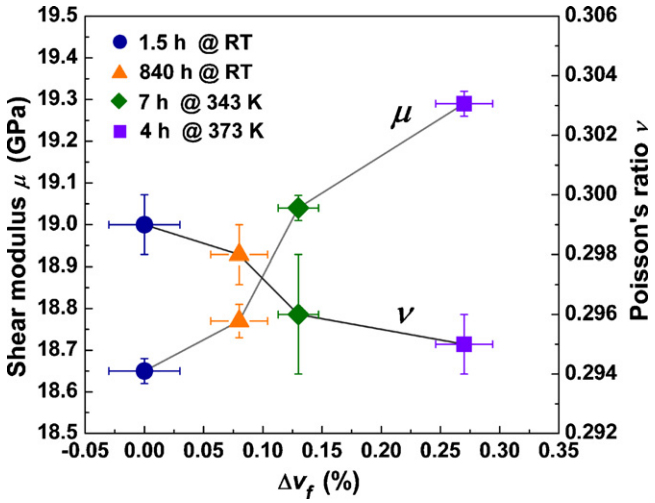

Fig. 5. Shear modulus (μ) and Poisson's ratio (ν) plotted as a function of free volume change ($\Delta\nu_f$) for the $Mg_{66}Zn_{30}Ca_4$ BMG at different relaxed states.

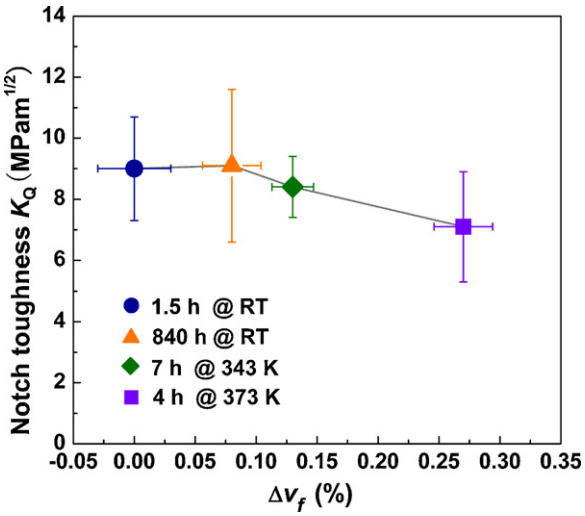

Fig. 7. Correlation between free volume change ($\Delta\nu_f$) and notch toughness (K_Q) of the $Mg_{66}Zn_{30}Ca_4$ BMG at different relaxed states.

of approximately 18.65 ± 0.02 GPa. With $\Delta\nu_f$ increasing via annealing, the μ of the sample increases, while the ν decreases gradually. When $\Delta\nu_f$ reaches 0.27% for the fully relaxed samples, μ and ν are 19.29 ± 0.03 GPa and 0.295 ± 0.001, increasing by 3.4% and decreasing by 1.4%, respectively, compared with the sample that annealed at T_R for 1.5 h.

3.3. Mechanical properties

Fig. 6 demonstrates the relationship of micro-hardness and $\Delta\nu_f$ for $Mg_{66}Zn_{30}Ca_4$ BMG at different relaxed states. It can be seen that with the increase in $\Delta\nu_f$ from 0 to 0.27%, the micro-hardness of the annealed samples gradually increases from 2.15 ± 0.04 GPa to 2.26 ± 0.04 GPa which corresponds to an increase of 5% by full relaxation.

Fig. 7 shows the K_Q of the rod samples versus the $\Delta\nu_f$ for the annealed $Mg_{66}Zn_{30}Ca_4$ BMG at different relaxed states. The high strength (~900 MPa) [12] of the samples places even the toughest samples in the plane strain regime, while the testing geometry produces failure under mode I loading condition. As seen in Fig. 7, the K_Q of the rod sample annealed at T_R for 1.5 h is 9.0 ± 1.7 $MPam^{1/2}$. With $\Delta\nu_f$ increasing by further relaxation, the K_Q value of the annealed samples are 9.1 ± 2.5 $MPam^{1/2}$ and 8.4 ± 1.0 $MPam^{1/2}$, which corresponds to the $\Delta\nu_f$ of 0.08% and 0.13%, respectively. For the fully relaxed samples with $\Delta\nu_f$ of 0.27%, the K_Q value retains a value of 7.1 ± 1.8 $MPam^{1/2}$. This result indicates that the notch toughness of the $Mg_{66}Zn_{30}Ca_4$ BMG is not very sensitive to further structural relaxation within a wide temperature and time range.

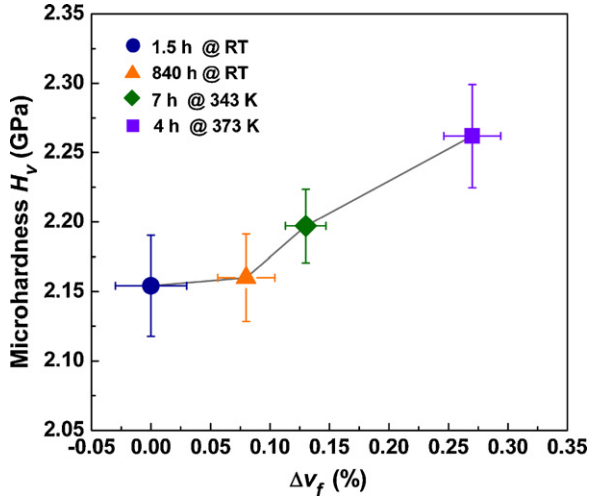

Fig. 6. Correlation between free volume change ($\Delta\nu_f$) and micro-hardness (H_v) of the $Mg_{66}Zn_{30}Ca_4$ BMG at different relaxed states.

Fig. 8(a) and (b) shows the SEM images of the fracture surfaces at low and high magnification of the $Mg_{66}Zn_{30}Ca_4$ BMG annealed at T_R for 1.5 h, respectively. The crack originates near the notch root and extends to the whole fracture surface. The higher magnification micrograph shows that a very fine vein pattern can be seen around the defects (pores or impurities) where the crack originated. With increasing distance away from the notch root, the vein-pattern morphology rapidly changes to a featureless mirror-like appearance, which is a typical morphology for brittle materials. Fig. 8(c) and (d) shows that the sample annealed at 373 K for 4 h has almost the same fracture surface morphology as the sample annealed at T_R for 1.5 h. This indicates that they have undergone almost the same process of fracture, which is consistent with their similar K_Q values.

K_Q values and fracture energy (G_Q) calculated using the relationship $G_Q = K_Q\,(1-\nu^2)/E$ as well as ΔH_t, ρ, and elastic moduli of the annealed $Mg_{66}Zn_{30}Ca_4$ BMG at different relaxed states are summarized in Table 1.

Recently, Lewandowski et al. [29] proposed a critical value of ν (0.31–0.32), or equivalently μ/B (0.41–0.43), at which a sharp brittle to tough transition occurs. Correlation of toughness/ductility with ν (or μ/B) for metallic glass is explained in terms of competition between shear and dilatation or competition between plastic flow and cleavage propagation that controls the fracture process in metallic glass. A higher ν decreases the potential energy of the shear transformation zone (STZ), thereby increasing the tendency of plastic deformation in mitigating fracture stress concentration [30].

For the purpose of comparison with various BMG classes, the G_Q obtained by notched samples testing is plotted against ν for Mg-[31], Cu-[32], Fe-[33,34] and Ti-based [35,36] BMGs reported in the previous literature with similar testing conditions (SENB test) and notch root radius (110–200 μm). For approximation, the blunting effect of notch root radius and geometry of the samples on fracture energy are ignored.

As seen in Fig. 9, higher values of ν mainly give higher G_Q for different BMGs. The G_Q of the $Mg_{66}Zn_{30}Ca_4$ BMG with the lowest ν values (<0.31–0.32) is only comparable to the lower bound of Fe-based BMGs, but significantly lower than that of Cu- and Ti-based

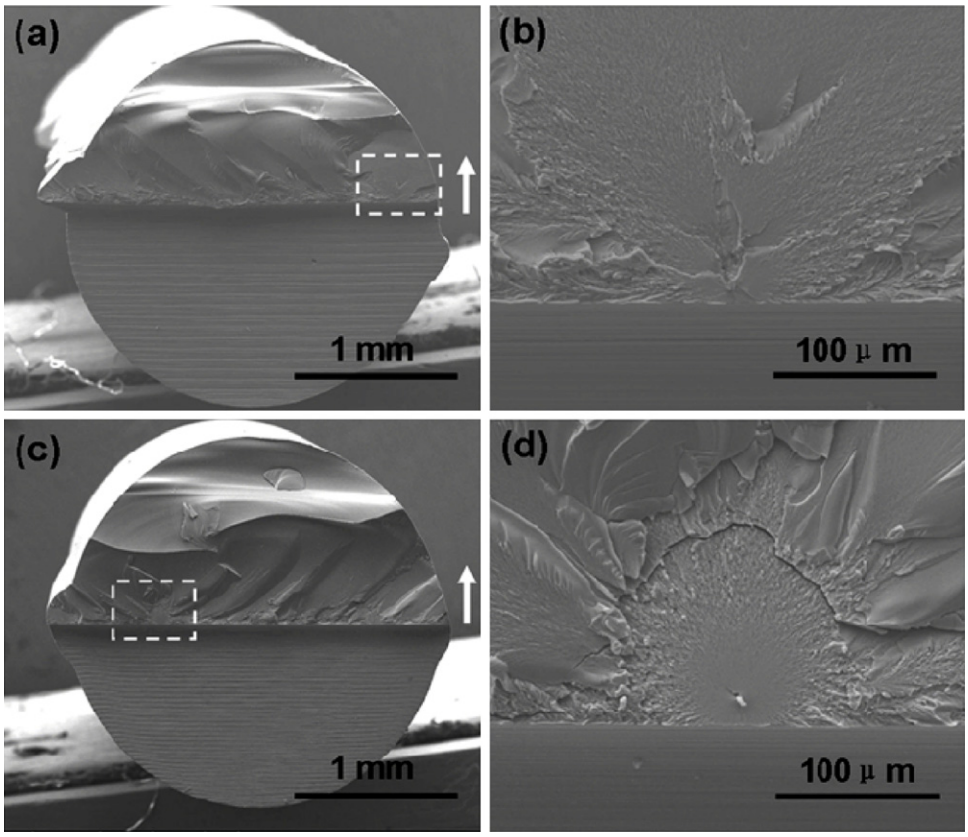

Fig. 8. SEM images of the fracture surface of the $Mg_{66}Zn_{30}Ca_4$ BMG at different relaxed states: (a) annealed at room temperature for 1.5 h and (c) annealed at 373 K for 4 h; (b) and (d) are higher magnification images of the marked regions in (a) and (c), respectively. The crack propagation direction is indicated by white arrows.

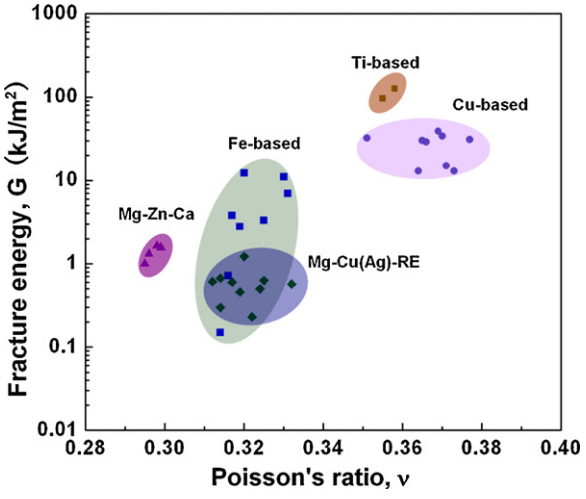

Fig. 9. Comparison of fracture energy (G) and Poisson's ratio (ν) of the Mg–Zn–Ca BMG with Mg–Cu (Ag)-RE BMG, Cu-based, Fe-based and Ti-based BMGs.

BMGs, which have the ν values much larger than the critical value (0.31–0.32). For the different Mg-based metallic glasses, although the $Mg_{66}Zn_{30}Ca_4$ BMG has a relatively lower ν, the measured G_Q is slightly higher than that of Mg–Cu(Ag)-RE BMGs. It is presumed that samples size also influences the measured G_Q values of these Mg-based BMGs because the notch toughness test samples for the Mg–Cu(Ag)-RE BMGs were obtained from the 4 mm diameter rods [31].

Structural relaxation is usually accompanied by severe embrittlement for most metallic glasses. However, in this work, the notch toughness of the $Mg_{66}Zn_{30}Ca_4$ BMG is not very sensitive to its structural relaxation over a wide temperature and time range. Similar results have also been reported in previous literature. Yavari [37] reported that, for the hypoeutectic $(Fe_{0.5}Ni_{0.5})_{83}B_{17}$ and $Fe_{83}B_{17}$ alloys, the glass ribbons remained fully ductile after annealing for 2 h at 573 K and 553 K, respectively. Recently, Yokoyama et al. [38,39] reported that the hypoeutectic $Zr_{60}Cu_{30}Al_{10}$ BMG also exhibited no degradation of ductility/toughness even after full structural relaxation, and the U-notched Charpy impact value of the hypoeutectic $Zr_{60}Cu_{30}Al_{10}$ BMG could even increase significantly by annealing just below the T_g. It was proposed that the heterogeneity of the glass structure might be a significant factor in the enhancement of plasticity and ductility for the hypoeutectic

Table 1
Enthalpy change (ΔH_t), mass density (ρ), Young's modulus (E), shear modulus (μ), bulk modulus (B), Poisson's ratio (ν), notch toughness (K_Q), and fracture energy (G_Q) of the $Mg_{66}Zn_{30}Ca_4$ BMG at different relaxed states.

Sample state	ΔH_t (kJ/mol)	ρ (g/cm^3)	E (GPa)	μ (GPa)	B (GPa)	ν	μ/B	K_Q (MPam$^{1/2}$)	G_Q (kJ/m^2)
RT for 1.5 h	0.07	2.9204	48.4 ± 0.1	18.65 ± 0.02	40.1 ± 0.3	0.299 ± 0.001	0.4654	9.0 ± 1.7	1.6 ± 0.6
RT for 840 h	0.29	2.9228	48.8 ± 0.3	18.77 ± 0.03	40.3 ± 0.2	0.298 ± 0.001	0.4658	9.1 ± 2.5	1.7 ± 0.8
343 K for 7 h	0.46	2.9243	49.4 ± 0.1	19.04 ± 0.03	40.4 ± 0.4	0.296 ± 0.001	0.4712	8.4 ± 1.0	1.3 ± 0.3
373 K for 4 h	0.68	2.9282	49.9 ± 0.3	19.29 ± 0.03	40.6 ± 0.2	0.295 ± 0.001	0.4757	7.1 ± 1.8	1.0 ± 0.5

$Zr_{60}Cu_{30}Al_{10}$ BMG. However, the possible mechanism may be different in Mg–Zn–Ca system since the $Mg_{66}Zn_{30}Ca_4$ alloy just locates at the eutectic composition correlated with a eutectic reaction of $L \rightarrow Mg + Ca_2Mg_5Zn_{13}$ [40].

As for other Mg-based BMGs, Castellero et al. [22] have reported that the bending strain of $Mg_{65}Cu_{25}Y_{10}$ ribbon showed an obvious ductile-to-brittle transition after annealing at T_R for 1 h to 3 h, and with increasing further the annealing time, the bending strain of $Mg_{65}Cu_{25}Y_{10}$ ribbon remained unchanged. The T_g of $Mg_{66}Zn_{30}Ca_4$ BMG is 387 K, which is much lower than that of $Mg_{65}Cu_{25}Y_{10}$ metallic glass (T_g = 420 K), indicating that the $Mg_{66}Zn_{30}Ca_4$ BMG may be more sensitive to room-temperature structural relaxation than the $Mg_{65}Cu_{25}Y_{10}$ metallic glass.

We noticed that the mechanical properties of $Mg_{66}Zn_{30}Ca_4$ BMG in the current study were mainly measured by the notch toughness test that needs a longer time (at least 1.5 h) to prepare the notched samples, thus the K_Q values of the samples annealed at T_R within 0 to 1.5 h could not be measured by the experiment.

Given this situation, it was presumed that the mechanical properties of the $Mg_{66}Zn_{30}Ca_4$ BMG might be also sensitive to room-temperature annealing and need an even shorter time (less than 1.5 h) to complete its ductile-to-brittle transition by annealing at T_R. Thus, even for the samples annealed at T_R for 1.5 h, the notch toughness tests were conducted after their ductile-to-brittle transition when the samples have become brittle. However, the notch toughness of the $Mg_{66}Zn_{30}Ca_4$ BMG was then not very sensitive to further structural relaxation within a wide temperature and time range.

Fig. 10 shows a plot of fracture toughness versus yield strength for several implant materials, including degradable polymethylmethacrylate (PMMA) [41], crystalline Mg alloys [42–44], natural bone [4,45], synthetic hydroxyapatite [4], and well-relaxed Mg–Zn–Ca BMG [12]. As seen in Fig. 10, even though there may have been a ductile-to-brittle transition by annealing at T_R within 1.5 h, the well-relaxed Mg–Zn–Ca BMG still has a good combination of the fracture toughness and yield strength in comparison with its counterparts. The Mg–Zn–Ca BMG has the highest yield strength together with the fracture toughness comparable with the values of natural bone and higher than that of PMMA and synthetic hydroxyapatite. This advantage of Mg–Zn–Ca BMG may further promote its possible clinical applications as a new kind of implant material.

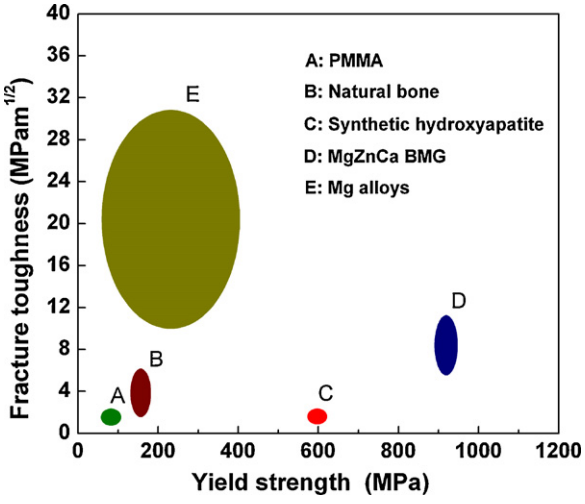

Fig. 10. Fracture toughness and yield strength of various implant materials in comparison with Mg–Zn–Ca BMG.

4. Conclusions

The current work investigated the structural relaxation at T_R and elevated temperature as well as its influence on the elastic properties and mechanical properties of $Mg_{66}Zn_{30}Ca_4$ BMG at different relaxed states. It was found that structural relaxation can occur even via room-temperature annealing. The structural relaxation of $Mg_{66}Zn_{30}Ca_4$ BMG results in increased μ and H_v and decreased ν. However, compared with the samples annealed at T_R for 1.5 h, the fully relaxed samples annealed at 373 K for 4 h did not show an obvious decrease in notch toughness. This finding indicates that the mechanical properties of the $Mg_{66}Zn_{30}Ca_4$ BMG are not very sensitive to its structural relaxation over a wide temperature and time range. Although the toughness values of the as-cast and fully relaxed Mg–Zn–Ca BMG are much lower than that of Ti- and Cu-based BMGs, they are comparable with most implant materials. Thus, $Mg_{66}Zn_{30}Ca_4$ BMG may be a promising implant material for future clinical applications.

Acknowledgements

This work was supported by the National Basic Research Program of China (973 Program) under contract No. 2007CB613906 and National Natural Science Foundation of China under Grant No. 51171180. The authors are very grateful to Prof. J. Xu and Dr. Q. Zheng for helpful discussions and advice.

References

[1] M. Niinomi, Metal. Mater. Trans. A 33 (2002) 477–486.
[2] F. Witte, V. Kaese, H. Haferkamp, E. Switzer, A. Meyer-Lindenberg, C.J. Wirth, H. Windhagen, Biomaterials 26 (2005) 3557–3563.
[3] F. Witte, J. Fischer, J. Nellesen, H.A. Crostack, V. Kaese, A. Pisch, F. Beckmann, H. Windhagen, Biomaterials 27 (2006) 1013–1018.
[4] M.P. Staiger, A.M. Pietak, J. Huadmai, G. Dias, Biomaterials 27 (2006) 1728–1734.
[5] L.P. Xu, G.N. Yu, E.L. Zhang, F. Pan, K. Yang, J. Biomed. Mater. Res. 83A (2007) 703–711.
[6] M.B. Kannan, R.K.S. Raman, Biomaterials 29 (2008) 2306–2314.
[7] Z.J. Li, X.N. Gu, S.Q. Lou, Y.F. Zheng, Biomaterials 29 (2008) 1329–1344.
[8] H.M. Wong, K.W.K. Yeung, K.O. Lam, V. Tam, P.K. Chu, K.D.K. Luk, K.M.C. Cheung, Biomaterials 31 (2010) 2084–2096.
[9] J.R. Scully, A. Gebert, J.H. Payer, J. Mater. Res. 22 (2007) 302–313.
[10] A. Gebert, U. Wolff, A. John, J. Eckert, L. Schultz, Mater. Sci. Eng. A 299 (2001) 125–135.
[11] X. Gu, G.J. Shiflet, F.Q. Guo, S.J. Poon, J. Mater. Res. 20 (2005) 1935–1938.
[12] Y.Y. Zhao, E. Ma, J. Xu, Scr. Mater. 58 (2008) 496–499.
[13] X.N. Gu, Y.F. Zheng, S.P. Zhong, T.F. Xi, J.Q. Wang, W.H. Wang, Biomaterials 31 (2010) 1093–1103.
[14] B. Zberg, P.J. Uggowitzer, J.F. Löffler, Nat. Mater. 8 (2009) 887–891.
[15] A.L. Greer, Structural relaxation and atomic transport in amorphous alloys, in: H.H. Liebermann (Ed.), Rapidly Solidified Alloys, Marcel Dekker, New York, 1993, p. 69.
[16] G.C. Chi, H.S. Chen, C.E. Miller, J. Appl. Phys. 49 (1978) 1715–1717.
[17] T.W. Wu, F. Spaepen, Philos. Mag. B 61 (1990) 739–750.
[18] J.J. Lewandowski, Mater. Trans. 42 (2001) 633–637.
[19] P. Murali, U. Ramamurty, Acta Mater. 53 (2005) 1467–1478.
[20] A. Niikura, A.P. Tsai, A. Inoue, T. Masumoto, J. Non-Cryst. Solids 159 (1993) 229–234.
[21] A. Castellero, D.I. Uhlenhaut, B. Moser, J.F. Löffler, Philos. Mag. Lett. 87 (2007) 383–392.
[22] A. Castellero, B. Moser, D.I. Uhlenhaut, F.H. Dalla Torre, J.F. Löffler, Acta Mater. 56 (2008) 3777–3785.
[23] D.I. Uhlenhaut, F.H. Dalla Torre, A. Castellero, C.A.P. Gomez, N. Djourelov, G. Krauss, B. Schmitt, B. Patterson, J.F. Löffler, Phil. Mag. 89 (2009) 233–248.
[24] G.Y. Yuan, K. Amiya, A. Inoue, J. Non-Cryst. Solids 351 (2005) 729–735.
[25] Y. Murakami, Stress Intensity Factors Handbook, Vol. 2, Pergamon, Oxford. UK, 1987, pp. 666.
[26] G.J. Fan, J.F. Löffler, R.K. Wunderlich, H.-J. Fecht, Acta Mater. 52 (2004) 667–674.
[27] A. van den Beukel, J. Sietsma, Acta Metall. Mater. 38 (1990) 383–389.
[28] A. Slipenyuk, J. Eckert, Scr. Mater. 50 (2004) 39–44.
[29] J.J. Lewandowski, W.H. Wang, A.L. Greer, Philos. Mag. Lett. 85 (2005) 77–87.
[30] S.J. Poon, A. Zhu, G.J. Shiflet, Appl. Phys. Lett. 92 (2008) 261902.
[31] S.G. Wang, L.L. Shi, J. Xu, J. Mater. Res. 26 (2011) 923–933.
[32] P. Jia, Z.D. Zhu, E. Ma, J. Xu, Scr. Mater. 61 (2009) 137–140.
[33] J.J. Lewandowski, X.J. Gu, A.S. Nouri, S.J. Poon, G.J. Shiflet, Appl. Phys. Lett. 92 (2008) 091918.

[34] M.D. Demetriou, G. Kaltenboeck, J.Y. Suh, G. Garrett, M. Floyd, C. Crewdson, D.C. Hofmann, H. Kozachkov, A. Wiest, J.P. Schramm, W.L. Johnson, Appl. Phys. Lett. 95 (2009) 041907.
[35] X.J. Gu, S.J. Poon, G.J. Shiflet, J.J. Lewandowski, Acta Mater. 58 (2010) 1708–1720.
[36] X.J. Gu, S.J. Poon, G.J. Shiflet, J.J. Lewandowski, Scr. Mater. 60 (2009) 1027–1030.
[37] A.R. Yavari, Mater. Sci. Eng. 98 (1988) 491–493.
[38] Y. Yokoyama, H. Fredriksson, H. Yasuda, M. Nishijima, A. Inoue, Mater. Trans. 48 (2007) 1363–1372.
[39] Y. Yokoyama, T. Yamasaki, P.K. Liaw, A. Inoue, Acta Mater. 56 (2008) 6097–6108.
[40] Y.Y. Zhao et al., unpublished results.
[41] M.R. Ayatollahi, A.R. Torabi, Mater. Des. 31 (2010) 60–67.
[42] K. Purazrang, K.U. Kainer, B.L. Mordike, Composites 22 (1991) 456–462.
[43] S. Barbagallo, E. Cerri, Eng. Fail. Anal. 11 (2004) 127–140.
[44] K. Lu, Science 328 (2010) 319–320.
[45] K.J. Koester, J.W. Ager, R.O. Ritchie, Nat. Mater. 7 (2008) 672–677.